Mechanistic insights of Epithelial Protein Lost in Neoplasm in prostate cancer metastasis

Collins RJ, Morgan LD, Owen S, Ruge F, Jiang WG, Sanders AJ

Author Affiliation: Cardiff China Medical Research Collaborative (CCMRC),

Cardiff University School of Medicine, Cardiff, UK

Manuscript type: Molecular Cancer Biology

Corresponding Author:

Dr Andrew Sanders

Cardiff China Medical Research Collaborative (CCMRC)

Cardiff University School of Medicine

Heath Park

Cardiff

CF14 4XN

SandersAJ1@cardiff.ac.uk

Tel: +44 29 2086 7074

Key words: EPLIN, prostate cancer, metastasis, Src, FAK

Novelty and Impact There is growing evidence to suggest EPLIN is a tumour suppressor molecule in several human cancers. The mechanisms governing this, however, are relatively unknown. This study provides insights into molecular associations which drive the regulatory actions of EPLIN, and establishes a broader picture of the signalling cascades co-ordinating cellular functions in prostate cancer. Developing a greater understanding of these cancer signalling systems will help elucidate better therapeutic strategies to prevent the progression of prostate cancer.

Abstract

EPLIN is frequently downregulated or lost in various cancers. The purpose of this study was to evaluate the importance of EPLIN in prostate cancer progression, with particular focus on the mechanistic implications to elucidate EPLIN's tumour suppressive function in cancer. EPLIN expression was evaluated in prostate cancer cell lines and tissues. PC-3 and LNCaP EPLINα overexpression models were generated through transfection with EPLINα sequence and EPLIN knockdown was achieved using shRNA in CA-HPV-10 cells. Functional assays were performed to evaluate cellular characteristics and potential mechanisms were evaluated using a protein microarray, and validated using western blot analysis. EPLIN expression was reduced in clinical prostate cancer sections, including hyperplasia ($p \leq 0.001$) and adenocarcinoma ($p=0.005$), when compared to normal prostate tissue. EPLINα overexpression reduced cell growth, migration and invasion, and influenced transcript, protein and phosphoprotein expression of paxillin, FAK and Src. EPLIN knockdown increased the invasive and migratory nature of CA-HPV-10 cells and also induced changes to FAK and Src total and/or phospho expression. Functional characterisation of cellular migration and invasion in addition to FAK and Src inhibition demonstrated differential effects between control and EPLINα overexpression and EPLIN knockdown cell lines. This study highlights that EPLIN expression in prostate cancer is able to influence several aspects of cancer cell characteristics, including cell growth, migration and invasion. The mechanism of the tumour suppressive action of EPLIN remains to be fully elucidated; and this study proposes a role for EPLIN's ability to regulate the aggressive characteristics of prostate cancer cells partially through regulating FAK/Src signalling.

Introduction

Prostate cancer is the second most common cancer in the UK and accounts for >11,000 cancer-related deaths (1). Epithelial protein lost in neoplasm (EPLIN) is a molecule that is frequently lost in cancer and has been implicated in the initiation of Epithelial Mesenchymal Transition (2), in addition to having tumour suppressive roles in cancer progression and development (2-6).

EPLIN was first reported in 1998 where differential expression was identified between normal epithelial cells and human papilloma virus (HPV) immortalized epithelial cells (7). EPLIN loss in cancer was demonstrated shortly after in oral, breast and prostate cancer (8). Subsequently, several publications have associated EPLIN to the progression and development of cancer (2, 4, 5, 9-11). EPLIN exists as two isoforms; a larger EPLINβ isoform consisting of 759 amino acids and a smaller EPLINα isoform of 600 amino acids (12). Although both isoforms display changes in expression in some cancers, the EPLINα isoform is generally considered more influential in cancer progression.

Several studies have begun to explore the potential mechanisms of EPLIN in cancer cell-related functions. EPLIN is linked to Extracellular signal-regulated kinase (ERK) signalling where ERK phosphorylates EPLIN at various sites contributing to actin filament reorganisation and enhancing cell migration (13). Epidermal growth factor (EGF) promotes EPLIN protein turnover via phosphorylation, ubiquitination and degradation; processes also linked to ERK1/2 signalling (14). The tumour suppressive molecule p53 has also been established as an EPLIN-targeting molecule for transcription, where induction of EPLIN can influence cancer cell characteristics, including cell invasion (15). The human phosphatase CDC14A has been identified as an EPLIN-targeting molecule by dephosphorylating EPLIN at two ERK-targeting

serine residues of EPLIN, counteracting the EGF-induced regulation of actin reorganisation, suggesting dynamic interplay of serine phosphorylation to drive EPLIN cell-related functions (16). Our lab and others have also established a potential link between EPLIN and paxillin, in addition to suggesting a role for EPLIN in the process of angiogenesis (4, 8, 11, 17). Taken together, EPLIN loss is likely to have significant effects on cellular functions including cellular migration, invasion and proliferation, thus exacerbating metastatic potential and cancer progression.

In the current study we provide functional evidence that EPLIN is a negative regulator of prostate cancer and acts as a tumour suppressive molecule to impede metastatic traits. We provide additional evidence supporting the downregulation of EPLIN in clinical prostate cancer and demonstrate a potential mechanistic link between EPLINα and Proto-oncogene tyrosine-protein kinase (Src) / Focal adhesion kinase (FAK) signalling.

Material and methods

Cell lines and conditions

Prostate cancer cell lines used for this study were purchased from ATCC (Middlesex, UK). PC-3, DU-145 and VCaP cells were cultured in Dulbecco's Modified Eagle's Medium (DMEM / Ham's F-12 with L-Glutamine) (Sigma-Aldrich, Dorset, UK), supplemented with antibiotics (Sigma-Aldrich, Dorset, UK) and 10% foetal calf serum (Sigma-Aldrich, Dorset, UK). LNCaP cells were cultured in RPMI-1640 medium (Sigma-Aldrich, Dorset, UK) supplemented with antibiotics (Sigma-Aldrich, Dorset, UK) and 10% foetal calf serum (Sigma-Aldrich, Dorset, UK). PZ-HPV-7 and CA-HPV-10 cells were cultured in keratinocyte serum free medium supplemented with 0.05mg/ml bovine pituitary extract and 5ng/ml EGF (Life Technologies, Paisley, UK). Cells were cultured at 37°C, 5% CO_2 in a humidified incubator.

Generation of prostate cancer cells overexpressing EPLINα.

A plasmid containing the expression sequence for EPLINα was constructed to mimic the full length EPLINα sequence as described previously (5). The plasmid was verified and used to transfect PC-3 and LNCaP prostate cancer cells. Cells with increased EPLINα expression were designated PC-3/LNCaP[EPLIN EXP], whilst control cells were designated PC-3/LNCaP[pEF6].

Knockdown of EPLIN using shRNA

EPLIN was knocked down using shRNA purchased from Santa Cruz Biotechnology (Santa Cruz Biotechnology, Texas, United States) and was performed according to manufacturer's instructions. Briefly, Solution A (containing shRNA plasmids) was

mixed 1:1 with Solution B (containing Plasmid Transfection Reagent) and mixed by pipetting before being left to incubate for 45 minutes at room temperature. For each transfection, 800µl of Plasmid Transfection Medium was added and 200µl of the shRNA Plasmid DNA/shRNA Plasmid Transfection Reagent Complex (Solution A + Solution B) giving a final volume of 1000µl to each well. Cells were incubated with shRNA for 8 hours at 37° C in a 5% CO_2 incubator. Following incubation, an additional 1000µl of cell media was added and left for a further 24 hours. Stable transfections were generated using puromycin selection at a concentration of 2.5µg/ml and subsequently maintained in maintenance media containing 0.25µg/ml puromycin until required.

RNA extraction, RT-PCR and cDNA synthesis

RNA extraction was performed according to the TRI reagent protocol (Sigma-Aldrich, Dorset, UK). RNA was reverse transcribed using a GoScript reverse transcription kit (Promega, Southampton, UK). Polymerase chain reaction (PCR) was subsequently performed to amplify EPLIN gene sequences using GoTaq Green Master Mix (Promega, Southampton, UK) and EPLIN specific primers (Table 1). Amplification conditions were as follows: 94°C for 5 min, 30 cycles of 94°C for 30s, 55°C for 30 s and 72°C for 40 s and a final extension of 72°C for 10 minutes. Products were separated on a 1% agarose gel stained with SYBR Safe Gel Stain (Life Technologies, Paisley, UK).

Protein extraction, quantification and western blotting

Cells were grown in T75 cell culture flasks until approximately 90% confluency, detached, lysed in lysis buffer and centrifuged. Protein concentration was subsequently determined using a Bio-Rad DC protein assay kit (Bio-Rad Laboratories, Hemel-Hempstead, UK). Protein analysis was performed using a standard sodium dodecyl sulfate-polyacrylamide gel electrophoresis (SDS-PAGE) and antibody steps were performed using the SNAP id® 2.0 Protein Detection System (Merck Millipore Ltd., Feltham, UK). EPLIN antibody was obtained from Bethyl Laboratories (Montgomery, Texas, USA). GAPDH, p-FAK Y397, p-c-Src Y530, p-Paxillin Y31, p-paxillin Y118, and p-FAK Y925 were from Insight Biotechnology (Middlesex, UK). Total paxillin and FAK were from BD Biosciences (BD Bioscience, Oxford, UK). C-Src and p-c-Src Y419 were from Abcam (Cambridge, UK). For knockdown experiments, FAK Y397, FAK Y925, paxillin Y31 and paxillin Y118 were obtained from Abcam (Cambridge, UK). Anti-mouse, anti-rabbit and anti-goat secondary antibodies were from Sigma-Aldrich (Dorset, UK).

In vitro **tumour cell functional assays**

Tumour cellular functional assays were performed to evaluate cellular proliferation, invasion and migration in PC-3 and LNCaP cells with manipulated EPLINα expression. Cell growth and invasion protocols were performed as previously reported (4). PC-3 cell migration was evaluated using a scratch/wound healing assay. PC-3 cells were seeded in a 24-well plate and allowed to reach confluence. Upon confluence, vertical scratches were made in the monolayer. Closure of the scratch was analysed over a 4 hour period under the microscope and images taken at 1 hour

intervals. Cellular migration was calculated at each time point based on wound closure in comparison to the time 0 image. LNCaP cell migration was evaluated using a transwell migration assay. LNCaP cells were seeded at a density of 50,000 cells into uncoated transwell inserts containing 8.0μm pores and placed into a 24 well plate. Following a 3 day period, cells that migrated through the pores were fixed in formalin and stained using crystal violet. For the LNCaP invasion assay, cells were seeded at a density of 60,000 cells per well. Cellular invasion and migration was also determined in the presence of an FAK inhibitor (CAS4506-66-5) (Santa Cruz Biotechnology, Texas, United States) at a concentration of 5μM, and a Src inhibitor (dasatinib) (Axon Medchem, Groningen, Netherlands) at a concentration of 500nM to determine the effect of EPLINα overexpression in conjunction with FAK/Src inhibition. For knockdown experiments, cellular migration and invasion was determined in control shRNA and EPLIN shRNA CA-HPV-10 cells. Cellular migration was evaluated using a transwell migration assay using the above protocol and a seeding density of 20,000 cells/well. For the invasion assay, the protocol was identical to the PC-3/LNCaP procedure also with a seeding density of 20,000 cells/well.

Protein microarray analysis

Protein was extracted from PC-3$^{EPLIN\ EXP}$ and PC-3^{pEF6} cells and quantified by fluorometric protein quantification, as reported previously (18), and subsequently sent to Kinexus^{TM} Bioinformatics (Kinexus Bioinformatics, Vancouver, British Columbia, Canada). Data was analysed using several parameters including Globally Normalised Signal Intensity, Z ratio and % Change from Control (CFC). A Z ratio greater than 1.64 or less than -1.64 was considered significantly up- or down-

regulated respectively. Molecules of interest were selected for validation using western blot analysis.

Tissue Microarray (TMA) analysis of prostate cancer tissue

Tissue Microarrays (TMA) were purchased to explore EPLIN expression in normal prostate tissue and prostate cancer tissue. TMA's were purchased from US Biomax (US Biomax, Inc., Rockville, USA) and tissues were collected under HIPAA approved protocols by the manufacturer. TMA's were stored and logged according to local HTA regulations. TMA1 was labelled HPro-Ade96Sur-01 and TMA2 was labelled PR8011a, according to the US Biomax reference numbers for each TMA.

Immunohistochemistry (IHC)

IHC was performed using anti-EPLIN antibody and the Vectastain® Elite Universal ABC Kit (Vector Labs, UK). Antigen retrieval was performed with 0.1M EDTA buffer for 20 minutes/full power in the microwave. Slides were allowed to cool in running tap water, before being blocked for two hours with 5-10% horse serum, and then incubated with primary antibody (2µg/ml) overnight at 4°C. After incubation with secondary and tertiary reagents from the kit, slides were developed with DAB (diaminobenzidine) (5mg/ml) substrate (Sigma-Aldrich, Dorset, UK) for 10 minutes, counterstained with Gill's haematoxylin, before being dehydrated, cleared in xylene and mounted in DPX (Sigma-Aldrich, Dorset, UK). Sections were visualized under a microscope and digital images were acquired. Staining intensities of EPLIN in each section were classified, by three independent researchers, as negative staining (0), weak staining (1), moderate staining (2) or strong staining (3) within epithelial components of the tissues. Staining intensities were subsequently aligned to patient/sample clinical information to identify differential staining patterns between groups.

Statistical analysis

Statistical analysis was performed using the SigmaPlot 11 (Systat Software Inc., London, UK) and Minitab 14 (Minitab Ltd., Coventry, UK) statistical software packages. Comparison between test groups was performed using a two sample, two tailed t-test or a Mann Whitney U test depending on data parameters. For PCR and western blot experiments, statistical significance was based on band intensities and was quantified using ImageJ software. All experiments were carried out a minimum of three independent times. Values of $p < 0.05$ were regarded as statistically significant.

Results

EPLIN expression is downregulated in prostate cancer cells

EPLIN transcript and protein expression were evaluated in one prostate and five prostate cancer cell lines (Figure 1A). EPLIN transcript was expressed in all cell lines with high levels seen in DU-145, CA-HPV-10 and PZ-HPV-7. Lowest levels of EPLIN transcript were seen in cell lines PC-3, LNCaP and VCaP. EPLINβ transcript was expressed at lower levels and remained relatively consistent throughout the cell lines. Given the relatively consistent levels of EPLINβ transcript within all samples, it can be concluded that PC-3, LNCaP and VCaP also had lowest levels of EPLINα expression as well as total EPLIN transcript expression. For protein analysis, highest expression of EPLINα and β was seen in CA-HPV-10 and EPLINα was moderately expressed in PZ-HPV-7. Lower EPLINα expression was also seen for DU-145 and VCaP, whilst EPLINβ was negative in all cell lines except CA-HPV-10. For PC-3 and LNCaP, both EPLIN isoforms were negative. For functional and mechanistic investigations, EPLINα expression was forced, utilising a construct coding for the alpha isoform only, in PC-3 and LNCaP cell lines and was knocked down in CA-HPV-10 cells using shRNA. PCR and western blot analyses demonstrated a significant increase in EPLIN/EPLINα expression in PC-3$^{\text{EPLIN EXP}}$ and LNCaP$^{\text{EPLIN}}$ $^{\text{EXP}}$ in comparison to the respective PC-3$^{\text{pEF6}}$ and LNCaP$^{\text{pEF6}}$ controls (Figure 1B/C), and this was more apparent at the protein level. Interestingly, enhancements in EPLINβ protein levels were also observed in both PC-3 and LNCaP cells that had been transfected with the EPLINα expression plasmid.

EPLIN expression is downregulated in prostate cancer tissue

EPLIN protein expression in clinical prostate cancer tissues was determined using two tissue microarrays (TMA) (HPRo-Ade96Sur-01 and PR8011a). EPLIN expression was scored based on the epithelial staining intensity of the samples (0, 1, 2, 3 representing, no, weak, moderate or strong staining respectively) by three independent researchers within each array. Patient clinical pathological information was considered alongside EPLIN expression. Within the first TMA (HPRo-Ade96Sur-01), EPLIN expression was reduced in cancer tissue compared to normal tissue, though this did not reach statistical significance following analysis of the assigned staining intensities (p=0.153) (Figure 1D). EPLIN expression in normal tissue was predominately expressed in the epithelial portion of the sections. In a second TMA (PR8011a; Figure 1E) EPLIN expression was significantly reduced in patients with prostate cancer hyperplasia (p≤0.001) and adenocarcinoma (p=0.005) compared to normal prostate tissue. A significant reduction in EPLIN expression was also seen in prostate cancer hyperplasia samples compared to adjacent prostate tissue (p=0.003) and close to significant reductions were seen between adjacent tissue and adenocarcinoma (p=0.054), and between normal prostate tissue and chronic inflammation (p=0.071). No significant differences were seen between normal prostate tissues and adjacent prostate tissue (p=0.422).

EPLIN loss in clinical prostate cancer was also seen following analysis of Gene Expression Omnibus (GEO) repositories from NCBI where EPLIN expression was significantly reduced in aggressive cancer tissues across several analyses (p<0.05) (Supplementary Figure 1A). In the HPRo-Ade96Sur-01 TMA, EPLIN staining intensities were also generally reduced in higher stage (Supplementary figure 1B)

and Gleason score (Supplementary Figure 1C) cancers, though neither trends were statistically significant (p=0.229 and 0.853 respectively).

EPLINα overexpression suppresses in vitro cell growth, migration and invasion of prostate cancer cells

PC-3$^{EPLIN\ EXP}$ cells had a significantly reduced growth rate compared to PC-3^{pEF6} cells at Day 3 (p=0.005) and at Day 5 (p=0.023) (Figure 2A). For the LNCaP cell line, a general reduction of cell growth was seen in LNCaP$^{EPLIN\ EXP}$ compared to LNCaP^{pEF6} cells, though significance was not reached (p=0.114 Day 3, p=0.329 Day 5) (Figure 2B). Cell invasiveness was determined using a Matrigel invasion assay. PC-3$^{EPLIN\ EXP}$ cells were significantly less invasive than control PC-3^{pEF6} cells (p=0.048) (Figure 2C). Similarly LNCaP$^{EPLIN\ EXP}$ cells were less invasive than control LNCaP^{pEF6} cells, though this was not significant (p=0.194) (Figure 2D). Cellular migration was assessed using a wound healing assay and demonstrated a significant reduction in PC-3$^{EPLIN\ EXP}$ cells at the 2 hour (p=0.011), 3 hour (p=0.004) and 4 hour (p=0.005) time points, compared to PC-3^{pEF6} control cells (Figure 2E). A transwell migration assay was also performed using the LNCaP cell model (Figure 2F) and revealed a general, though non-significant reduction of cellular migration in LNCaP$^{EPLIN\ EXP}$ cells compared to LNCaP^{pEF6} cells (p=0.381).

EPLINα expression induces changes to paxillin and FAK expression/phosphorylation

EPLINα overexpression increased the expression of FAK transcript in PC-3 and LNCaP cells lines, with a significant increase observed in PC-3$^{EPLIN\ EXP}$ cells compared to PC-3^{pEF6} controls (p=0.01) (Figure 3A). EPLINα overexpression had no effect on paxillin transcript expression in the PC-3 cell line, and significantly

reduced paxillin in LNCaP$^{EPLIN\ EXP}$ compared to LNCaP^{pEF6} (p<0.001). EPLINα overexpression also induced several changes to FAK/paxillin phospho- and protein expression (Figure 3B). In the PC-3 cell model, EPLINα overexpression significantly increased the expression of pFAK Y925 (Supplementary Figure 2A; p=0.01), pPaxillin Y31 (Supplementary Figure 2B; p=0.031), total paxillin (Supplementary Figure 2C; p<0.001), and pPaxillin Y118 (Supplementary Figure 2D; p=0.026) in comparison to control PC-3^{pEF6} cells. Increased expression of total FAK and pFAK Y397 were noted in PC-3 cells following EPLINα overexpression, though these were not found to be significant (p>0.05). In the LNCaP cell model, EPLINα overexpression caused a significant increase in the expression of pFAK Y397 (Supplementary Figure 2E; p=0.036) and a significant reduction of pPaxillin Y118 (Supplementary Figure 2F; p=0.023) when compared to LNCaP^{pEF6} control cells. No significant differences between LNCaP^{pEF6} and LNCaP$^{EPLIN\ EXP}$ were seen for total FAK, pFAK Y925, total paxillin and pPaxilln Y31 (p>0.05).

EPLINα may influence cellular migration and invasion partly through the action of FAK in PC-3 cells

To explore the functional relationship between EPLINα and FAK, *in vitro* tumour invasion and migration assays were performed in PC-3 and LNCaP cells in the presence of an inhibitor known to inhibit FAK activity. For the invasion assay, treatment of PC-3^{pEF6} cells with 5μM FAK inhibitor significantly reduced cellular invasion (p=0.034 vs untreated PC-3^{pEF6} cells), but no significant differences were noted for PC-3$^{EPLIN\ EXP}$ cells (p>0.05 vs. untreated PC-3$^{EPLIN\ EXP}$) (Figure 3C). In LNCaP cells, FAK inhibition generally reduced cellular invasion of both LNCaP^{pEF6} and LNCaP$^{EPLIN\ EXP}$ cells, but significance was not reached for either condition (Figure 3D).

In PC-3^{pEF6} cells, treatment with FAK inhibitor (5µM) significantly reduced cellular migration, assessed using a wound healing assay, at 2, 3 and 4 hour time points (p=0.003, p=0.002 and p=0.001, respectively vs. untreated PC-3^{pEF6}) (Figure 3E; Top). Treatment of PC-3$^{EPLIN\ EXP}$ cells with FAK inhibitor (5µM) lead to a significant decrease in cellular migration at 3 hours (p=0.034 vs. untreated PC-3$^{EPLIN\ EXP}$ cells), though no other significant differences were seen (p>0.05 vs untreated PC-3$^{EPLIN\ EXP}$ for hours 1, 2 and 4) (Figure 3E; bottom). In LNCaP^{pEF6} (Figure 3F; top) and in LNCaP$^{EPLIN\ EXP}$ (Figure 3F; bottom) cells, FAK inhibition reduced cell migration, assessed using a transwell assay, though this impact was only found to be significant, in comparison to respective untreated controls, in LNCaP$^{EPLIN\ EXP}$ cells (p=0.01).

EPLINα overexpression negatively regulates Src in prostate cancer cells

A protein microarray was performed on PC-3^{pEF6} and PC-3$^{EPLIN\ EXP}$ cells to highlight molecules whose expression or phosphorylation status was influenced by forced expression of EPLINα. The protein microarray contained three pan-specific and two phospho-specific (Y529 and Y419) antibodies for Src. No significant differences between PC-3^{pEF6} and PC-3$^{EPLIN\ EXP}$ cells were seen in total Src expression or p-SrcY529 expression, with Z-ratios remaining between 1.64 and -1.64. Of interest, a key Src activation site, Y419 was significantly down-regulated in PC-3$^{EPLIN\ EXP}$ cells compared to PC-3^{pEF6} cells (z-ratio < -1.64, Figure 4A). To further assess this relationship we sought to verify this trend using western blot analysis in PC-3 and LNCaP cell lines (Figure 4B). A decrease in band intensity for p-Src Y419 was seen which, following semi-quantitative analysis and normalisation to GAPDH, was found to be significantly downregulated in PC-3$^{EPLIN\ EXP}$ cells compared to PC-3^{pEF6} cells (Figure 4C; p=0.005). A reduction of p-Src Y419 was also seen in LNCaP^{EPLIN}

^{EXP} cells compared to LNCaP^{pEF6} cells, however this change was not statistically significant (p>0.05). In addition to p-Src Y419, total Src and p-Src Y530 were also tested. For both PC-3 and LNCaP cells, no significant differences were seen in total Src expression, which is in keeping with the results of the microarray. Contrary to p-Src Y419, and partially to that of the protein microarray, p-Src Y530, a common site of dephosphorylation, was found to be enhanced via western blotting following EPLINα overexpression in PC-3 cells (Figure 4D; p=0.027 vs. PC-3^{pEF6} cells). In LNCaP, p-Src Y530 was also increased when EPLINα was overexpressed (Figure 4B), however the increase didn't quite reach significance following semi-quantitative band analysis and normalisation to GAPDH (p=0.068) (Figure 4E).

Negative regulation of Src by EPLINα influences the invasive phenotype of prostate cancer cells

To further elucidate the association of EPLINα and Src, two *in vitro* tumour cell functional assays were performed in the presence of a Src inhibitor (500nM dasatinib). In PC-3^{pEF6} cells, dasatinib treatment caused a significant reduction of cellular invasion (p<0.001 vs. untreated PC-3^{pEF6}). However, this trend was not observed in PC-3$^{EPLIN\ EXP}$ cells, and treatment of dasatinib offered no further reductions in invasion in this cell line (p > 0.05 vs. untreated PC-3$^{EPLIN\ EXP}$ cells) (Figure 5A). The impact of combined EPLINα overexpression and Src inhibition on PC-3 migration was also assessed using a scratch wound assay. Dasatinib treatment caused a significant reduction in the migratory rates of PC-3^{pEF6} cells following a 4 hour time period (p=0.004 vs. untreated PC-3^{pEF6} cells). In PC-3$^{EPLIN\ EXP}$ cells, cellular migration was also significantly reduced at the four hour time point when dasatinib was used, though not to as great an extent (p=0.012 vs. untreated PC-3^{EPLIN} ^{EXP} cells) (Figure 5B). The impact of dasatinib was also tested in the LNCaP cell

model using an *in vitro* invasion assay and a transwell migration assay (Figure 5C/D). For untreated LNCaP cells, EPLINα overexpression reduced cellular invasion as previously observed, and in this instance reached statistical significance (p=0.015 vs LNCaP^{pEF6} cells) (Figure 5C). Dasatinib treatment caused a significant reduction in the cellular invasion of LNCaP^{pEF6} cells (p=0.016 vs. untreated LNCaP^{pEF6} cells) (Figure 5C). However, similar to the PC-3 model, treatment of LNCaP$^{EPLIN\ EXP}$ cells with dasatinib had no further significant effects on cellular invasion (p>0.05 vs. untreated LNCaP$^{EPLIN\ EXP}$ cells) (Figure 5C). Finally, dasatinib treatment significantly reduced the cellular migration of both LNCaP^{pEF6} cells and LNCaP$^{EPLIN\ EXP}$ cells (p<0.001 compared to respective untreated controls), but did not appear to have any differential effects between the two lines (Figure 5D).

EPLIN knockdown in CA-HPV-10 cells influenced the expression Src and FAK

EPLIN was knocked down in CA-HPV-10 cells using shRNA and the impact of EPLIN suppression was explored in relation to paxillin, FAK and Src expression (Figure 6). EPLIN transcript expression was significantly reduced using shRNA and verified by conventional PCR and semi-quantitative analysis (p=<0.001) (Figure 6A). EPLINα protein expression was also significantly reduced and verified by western blotting and semi-quantitative analysis (p=0.004) (Figure 6B). No significant changes were seen in total paxillin, paxillin Y31, paxillin Y118, FAK Y925, total Src and Src Y530 following EPLIN knockdown in CA-HPV-10 cells (Figure 6C/D/E). However, EPLIN knockdown significantly increased the expression of total FAK in CA-HPV-10 cells (p=0.002) (Figure 6D/Supplementary Figure 3A) and appeared to increase the expression of FAK Y397 in CA-HPV-10, although significance was not reached (p=0.162) (Figure 6D/Supplementary Figure

3B). EPLIN knockdown also significantly increased the expression of Src Y419 in CA-HPV-10 cells (p=0.008) (Figure 6E/Supplementary Figure 3C).

Functional significance of EPLIN knockdown in CA-HPV-10 and links to FAK and Src

The impact of EPLIN suppression individually and in conjunction with FAK or Src inhibition on cellular invasion (Figure 6F) and migration (Figure 6G) was explored in the CA-HPV-10 model. Knockdown of EPLIN brought about a significant increase in CA-HPV-10 cellular invasion (p=0.006). Inhibition of Src using dasatinib (500nM) has similar effects on both control and EPLIN knockdown CA-HPV-10 cells, causing significant decreases in invasion in comparison to the relative untreated lines (both p=<0.001). Interestingly, the addition of an FAK inhibitor (5µM) had differential effects, having no significant effects on control CA-HPV-10 cells but significantly reducing invasion in EPLIN knockdown CA-HPV-10 cells (p=0.017 vs. untreated EPLIN knockdown CA-HPV-10 cells) (Figure 6F). A similar trend was also observed in relation to cellular migration (Figure 6G). EPLIN knockdown significantly increased the migration of CA-HPV-10 cells using a transwell system (p=<0.001) and inhibition of Src induced significant decreases in migration in both CA-HPV-10 control and CA-HPV-10 EPLIN knockdown cells (both p=<0.001 vs. relative untreated equivalent). FAK inhibition again had differential impacts on CA-HPV-10 control and EPLIN knockdown cells, where no significant changes in migration were seen in control cells, whereas for CA-HPV-10 EPLIN knockdown cells, cellular migration was significantly decreased when FAK was inhibited (p=0.004 vs. untreated CA-HPV-10 EPLIN knockdown cells) (Figure 6G).

Discussion

Previous studies evaluating EPLIN in cancer progression have identified loss of EPLIN in aggressive cancer and suggest a regulatory role for EPLIN as a tumour suppressor (2, 4-6, 9, 10). Additionally, several mechanisms have been reported for the regulation of EPLIN expression, including ERK (13), EGF (14), DNp73 (19) and p53 (15) and provide important insight into how EPLIN may be regulated at a functional or expressional level. The aim of this study was to explore the importance of EPLIN in the progression and development of prostate cancer, with particular emphasis on elucidating mechanisms through which EPLIN inhibits prostate cancer progression to aid in the design of novel therapeutic strategies.

Protein and transcript analysis in normal and cancerous prostate cell lines revealed EPLIN is differentially expressed in prostate cancer, with a reduction of EPLIN expression generally coinciding with aggressiveness of the cell line. This concurs with previous reports using PC-3 and LNCaP where EPLINα is lost in aggressive prostate cancer (8). We also explored the clinical implications of EPLIN expression suggesting that EPLIN expression is reduced or lost during progression of prostate cancer. Taken together with other studies (2, 4, 5, 10), our data suggests EPLIN could be useful as a potential prognostic marker for prostate cancer progression, however more in depth investigation, utilising larger cohorts are required to fully clarify this.

Interestingly, following overexpression of EPLINα in the cellular based assays, we also saw an enhanced protein expression of EPLINβ. The exact reason for this is currently unknown, though, given that the expression sequence used in the cellular transfections does not contain coding regions for EPLINβ, nor did it significantly enhance the transcript expression of this isoform, we anticipate this may be a result

of enhanced stabilisation or translation of the EPLINβ isoform. EPLINα overexpression reduced cellular growth of PC-3 cells, and this is in keeping with both *in vitro* and *in vivo* observations from a previous study conducted in the host laboratory (4). Previously, we have demonstrated a reduction of cellular growth in a sub cutaneous mouse model which corroborates our work detailed here on cellular proliferation (4). The work here substantiates EPLINα's role as a suppressor of cell growth in prostate cancer (4) and other cancers including oesophageal cancer (10) and breast cancer (5). PC-3 and LNCaP EPLINα overexpression models were less able to infiltrate and invade a Matrigel membrane, an observation again in keeping with previous data in PC-3 (4) and LNCaP (2) models, and in lung and breast cancer (15) where EPLIN expression was able to influence cancer cell invasiveness. The migration assays in this study corroborates previous work elucidating EPLINα in tumour cellular migration in endothelial cells (11) and in breast cancer cells (5). Taken together, our current data supports a metastasis suppressive role for EPLINα in prostate cancer. Although future animal studies using *in vivo* metastasis models are needed to further explore the anti-metastatic impact of EPLIN in complex systems, this study highlights the potential for use in therapy to influence various cancer cell-related functions.

The EPLIN interactome has only been explored briefly in the last decade, and the mechanisms governing how EPLIN exerts these tumour suppressive functions isn't fully understood. As part of this study we aimed to explore the relationship between EPLINα, paxillin and FAK and the potential of such a relationship to drive the anti-metastatic role of EPLINα. EPLINα overexpression influenced paxillin and FAK expression and also the phosphorylation of certain key residues within these proteins, such as FAK Y397/Y925 and paxillin Y31/Y118. These regions are critical

to paxillin and FAK function and have implications for cellular migration and cancer progression (20). EPLINα overexpression enhanced paxillin phosphorylation at Y31/Y118 in PC-3 cells and phosphorylation within these residues have been associated with differential effects on cellular migration (21, 22), and hence reveals potential mechanisms through which EPLINα can regulate cellular migration. In contrast, LNCaP cells showed a reduction of paxillin Y118 following EPLINα overexpression and EPLIN suppression in CA-HPV-10 cells did not significantly influence paxillin or phospho-paxillin expression. If EPLIN can affect paxillin Y31/Y118 phosphorylation in cancer, depending on cell type, this could also lead to differential effects on paxillin:FAK association, thus resulting in changes to a number of cellular processes such as cellular migration and invasion (23). Whilst these findings are intriguing, care must be taken when interpreting the data, particularly for the LNCaP model, as there is a discrepancy between the paxillin transcript and protein effect following EPLIN overexpression, therefore further work is required to fully validate this link. FAK Y397 is a region of FAK crucial for controlling cellular functions, including cell survival and cellular migration (24), co-ordinating interaction with regulatory proteins, like phosphoinositide 3-kinase (PI3K) (25), and is a major binding site for the SH2 domain of Src family kinases (26). Y925 is an established region of FAK and is important for cell migration, focal adhesion turnover and cell protrusion (27). Forced EPLINα expression also exerted differential effects of FAK Y397 and Y925 in the two cell lines tested, suggesting the EPLIN and FAK associations could be cell type specific. FAK inhibition using an FAK Y397 inhibitor was less effective at reducing cellular migration of PC-3 cells overexpressing EPLINα, compared to PC-3[pEF6] control cells, though this trend was not so clear in LNCaP cells. Interestingly, using a CA-HPV-10 knockdown

model, differential effects on invasion and migration were again observed between control and EPLIN suppressed cells where inhibition of FAK in control cells, expressing higher levels of EPLIN, had no impact on invasion or migration, whereas in EPLIN knockdown cells, these traits were further reduced. Again similar to PC-3 and LNCaP EPLIN overexpression cells, CA-HPV-10 EPLIN knockdown cells displayed generally higher levels of total FAK and FAK Y397. Whilst the expressional differences brought about by EPLIN overexpression or suppression are difficult to explain, the functional impact appears to be more consistent, suggesting that higher EPLIN expression exerts a level of negative regulation on FAK and subsequent loss of EPLIN removes such control, enhancing the sensitivity to FAK inhibition on migration and invasion. Whilst our data suggests that manipulation of EPLIN also impacts expressional and phosphorylation changes of FAK, the precise mechanism through which it brings about this effect appears complex, potentially arising due to differing cell models or differences in transfection efficiencies. Taken together our data highlights a potential regulatory association between EPLIN, FAK and paxillin however, further research is required to fully clarify this association and regulatory mechanism. It is particularly interesting to consider that EPLINα may also act upstream/downstream of FAK, potentially targeting this pathway at a number of points through its action on Src, a molecule which associates with FAK at Y397 to phosphorylate several other regions of FAK to propagate various signalling mechanisms (28, 29). The protein microarray demonstrated that EPLINα overexpression in PC-3 cells induced a reduction of Src Y419 phosphorylation, a region of Src considered to be the classical activation domain, associated with the progression of various cancers and linked to function and catalytic activity (30). This link was then explored using our CA-HPV-10 model, where knockdown of EPLIN

increased the expression of Src Y419. Our current data suggests that EPLINα is a negative regulator of Src signalling, through direct or indirect phosphorylation/dephosphoylation of Src Y419 and/or Src Y530. Src is commonly elevated in cancer and is synergistic with paxillin and FAK, and propagation of this pathway is generally associated with cancer progression (31). Elevations in Src activity are also associated with activation of proteins involved in the mitogen activated protein kinase (MAPK) pathway to co-ordinate various cellular functions and control gene expression (32). In addition, Src phosphorylates β-catenin and suppresses the association of β-catenin with E-cadherin at adherens junctions, disrupting the integrity of adherens junctions and driving epithelial to mesenchymal transition (EMT) (33). EPLIN has previously been postulated as a suppressor of EMT in prostate cancer through the suppression of E-cadherin (2). Elevated Src activity in cancer is also linked to increased cellular invasion and progression-related events like EMT (34), influences actin dynamics and invasion (35) and has been implicated in cancer cell migration and invasion to a bone derived microenvironment (36). Src activity is also associated with cell cycle arrest (37), has implications on cellular functions in triple negative breast cancer (38) and has significance in prostate cancer progression (39). Finally, expression of Src is associated with FAK activity and specifically monitors focal adhesion dynamics to control cellular functions like migration and focal adhesion turnover (40, 41). Cells with altered focal adhesion turnover leads to less effective cellular migration, locomotion and spreading of cells, so this highlights potential mechanisms to which EPLIN can regulate cellular migration (42). The use of the dasatinib Src inhibitor partially corroborated these findings, particularly when evaluating EPLINα overexpression and Src activity in relation to cellular invasion where enhanced EPLINα expression

reduced the anti-invasive impact of Src inhibition. However, unfortunately this trend was not replicated in the CA-HPV-10 knockdown model, where Src inhibition had similar effects on both control and EPLIN suppressed cells. These differences may have resulted due to the different model systems used. For example, enhancing the regulation through EPLIN overexpression, may bring about more significant effects than removal of this regulation through knockdown. Alternatively this may have arisen due to the differing nature and expressional profiles of the cell models themselves. Despite this, the current study has highlighted the ability of EPLIN manipulation to alter Src expression in the cell lines tested here. Inhibition of Src is already an established area of therapeutics for cancer biology (43) and loss of EPLIN has previously been associated with enhanced chemoresistance to docetaxel and doxorubicin (2). Together, this presents interesting avenues of future work exploring the impact of EPLIN on cancer sensitivity to a range of chemotherapeutic agents and further scientific study of this relationship is warranted.

The current study has demonstrated that EPLINα is able to regulate the expression and phosphorylation of paxillin, FAK and Src in prostate cancer, and in doing so potentially regulate a large number of cellular characteristics. However, key clinical questions remain, such as how to retain or replace EPLINα expression in aggressive cancer cells. This area of EPLIN biology remains in its infancy though recently it was reported that a small molecule inhibitor was able to enhance EPLINα protein expression, an effect linked to the suppressive action of p53 in cancer (15). Identification of compounds such as these and their use in conjunction with anti-FAK/Src molecular therapies could represent promising novel therapeutic strategies.

Acknowledgements

Conflict of interest

The authors declare no conflict of interest.

References

1.   CancerResearchUK. Prostate cancer statistics 2017 [cited 2016 12/5/16]. Available from: http://www.cancerresearchuk.org/health-professional/cancer-statistics/statistics-by-cancer-type/prostate-cancer.

2.   Zhang S, Wang X, Osunkoya AO, Iqbal S, Wang Y, Chen Z, et al. EPLIN downregulation promotes epithelial-mesenchymal transition in prostate cancer cells and correlates with clinical lymph node metastasis. Oncogene. 2011;30(50):4941-52.

3.   Maul RS, Song Y, Amann KJ, Gerbin SC, Pollard TD, Chang DD. EPLIN regulates actin dynamics by cross-linking and stabilizing filaments. The Journal of cell biology. 2003;160(3):399-407.

4.   Sanders AJ, Martin TA, Ye L, Mason MD, Jiang WG. EPLIN is a negative regulator of prostate cancer growth and invasion. The Journal of urology. 2011;186(1):295-301.

5.   Jiang WG, Martin TA, Lewis-Russell JM, Douglas-Jones A, Ye L, Mansel RE. Eplin-alpha expression in human breast cancer, the impact on cellular migration and clinical outcome. Molecular cancer. 2008;7:71.

6.   Collins RJ, Jiang WG, Hargest R, Mason MD, Sanders AJ. EPLIN: a fundamental actin regulator in cancer metastasis? Cancer metastasis reviews. 2015;34(4):753-64.

7.   Chang DD, Park NH, Denny CT, Nelson SF, Pe M. Characterization of transformation related genes in oral cancer cells. Oncogene. 1998;16(15):1921-30.

8.   Maul RS, Chang DD. EPLIN, epithelial protein lost in neoplasm. Oncogene. 1999;18(54):7838-41.

9.   Liu R, Martin TA, Jordan NJ, Ruge F, Ye L, Jiang WG. Epithelial protein lost in neoplasm-alpha (EPLIN-alpha) is a potential prognostic marker for the progression of epithelial ovarian cancer. International journal of oncology. 2016;48(6):2488-96.

10.   Liu Y, Sanders AJ, Zhang L, Jiang WG. EPLIN-alpha expression in human oesophageal cancer and its impact on cellular aggressiveness and clinical outcome. Anticancer research. 2012;32(4):1283-9.

11.   Sanders AJ, Ye L, Mason MD, Jiang WG. The impact of EPLINalpha (Epithelial protein lost in neoplasm) on endothelial cells, angiogenesis and tumorigenesis. Angiogenesis. 2010;13(4):317-26.

12.   Chen S, Maul RS, Kim HR, Chang DD. Characterization of the human EPLIN (Epithelial Protein Lost in Neoplasm) gene reveals distinct promoters for the two EPLIN isoforms. Gene. 2000;248(1-2):69-76.

13.   Han MY, Kosako H, Watanabe T, Hattori S. Extracellular signal-regulated kinase/mitogen-activated protein kinase regulates actin organization and cell motility by phosphorylating the actin cross-linking protein EPLIN. Molecular and cellular biology. 2007;27(23):8190-204.

14.   Zhang S, Wang X, Iqbal S, Wang Y, Osunkoya AO, Chen Z, et al. Epidermal growth factor promotes protein degradation of epithelial protein lost in neoplasm (EPLIN), a putative metastasis suppressor, during epithelial-mesenchymal transition. The Journal of biological chemistry. 2013;288(3):1469-79.

15.   Ohashi T, Idogawa M, Sasaki Y, Tokino T. p53 mediates the suppression of cancer cell invasion by inducing LIMA1/EPLIN. Cancer letters. 2017;390:58-66.

16.   Chen NP, Uddin B, Hardt R, Ding W, Panic M, Lucibello I, et al. Human phosphatase CDC14A regulates actin organization through dephosphorylation of epithelial protein lost in neoplasm. Proceedings of the National Academy of Sciences of the United States of America. 2017;114(20):5201-6.

17.   Tsurumi H, Harita Y, Kurihara H, Kosako H, Hayashi K, Matsunaga A, et al. Epithelial protein lost in neoplasm modulates platelet-derived growth factor-mediated adhesion and motility of mesangial cells. Kidney international. 2014;86(3):548-57.

18.   Feng Y, Sanders AJ, Morgan LD, Owen S, Ruge F, Harding KG, et al. In vitro significance of SOCS-3 and SOCS-4 and potential mechanistic links to wound healing. Scientific reports. 2017;7(1):6715.

19.   Steder M, Alla V, Meier C, Spitschak A, Pahnke J, Furst K, et al. DNp73 exerts function in metastasis initiation by disconnecting the inhibitory role of EPLIN on IGF1R-AKT/STAT3 signaling. Cancer cell. 2013;24(4):512-27.

20.   Brown MC, Turner CE. Paxillin: adapting to change. Physiological reviews. 2004;84(4):1315-39.

21.   Petit V, Boyer B, Lentz D, Turner CE, Thiery JP, Valles AM. Phosphorylation of tyrosine residues 31 and 118 on paxillin regulates cell migration through an association with CRK in NBT-II cells. The Journal of cell biology. 2000;148(5):957-70.

22.   Yano H, Uchida H, Iwasaki T, Mukai M, Akedo H, Nakamura K, et al. Paxillin alpha and Crk-associated substrate exert opposing effects on cell migration and contact inhibition of growth through tyrosine phosphorylation. Proceedings of the National Academy of Sciences of the United States of America. 2000;97(16):9076-81.

23.   Deramaudt TB, Dujardin D, Noulet F, Martin S, Vauchelles R, Takeda K, et al. Altering FAK-paxillin interactions reduces adhesion, migration and invasion processes. PloS one. 2014;9(3):e92059.

24.   Hanks SK, Ryzhova L, Shin NY, Brabek J. Focal adhesion kinase signaling activities and their implications in the control of cell survival and motility. Frontiers in bioscience : a journal and virtual library. 2003;8:d982-96.

25.   Chen HC, Appeddu PA, Isoda H, Guan JL. Phosphorylation of tyrosine 397 in focal adhesion kinase is required for binding phosphatidylinositol 3-kinase. The Journal of biological chemistry. 1996;271(42):26329-34.

26.   Eide BL, Turck CW, Escobedo JA. Identification of Tyr-397 as the primary site of tyrosine phosphorylation and pp60src association in the focal adhesion kinase, pp125FAK. Molecular and cellular biology. 1995;15(5):2819-27.

27.   Deramaudt TB, Dujardin D, Hamadi A, Noulet F, Kolli K, De Mey J, et al. FAK phosphorylation at Tyr-925 regulates cross-talk between focal adhesion turnover and cell protrusion. Molecular biology of the cell. 2011;22(7):964-75.

28.   Schaller MD, Hildebrand JD, Shannon JD, Fox JW, Vines RR, Parsons JT. Autophosphorylation of the focal adhesion kinase, pp125FAK, directs SH2-dependent binding of pp60src. Molecular and cellular biology. 1994;14(3):1680-8.

29.   McLean GW, Carragher NO, Avizienyte E, Evans J, Brunton VG, Frame MC. The role of focal-adhesion kinase in cancer - a new therapeutic opportunity. Nature reviews Cancer. 2005;5(7):505-15.

30.   Cartwright CA, Meisler AI, Eckhart W. Activation of the pp60c-src protein kinase is an early event in colonic carcinogenesis. Proceedings of the National Academy of Sciences of the United States of America. 1990;87(2):558-62.

31.   Mitra SK, Schlaepfer DD. Integrin-regulated FAK-Src signaling in normal and cancer cells. Current opinion in cell biology. 2006;18(5):516-23.

32.   Turner CE. Paxillin and focal adhesion signalling. Nature cell biology. 2000;2(12):E231-6.

33.   Behrens J, Vakaet L, Friis R, Winterhager E, Van Roy F, Mareel MM, et al. Loss of epithelial differentiation and gain of invasiveness correlates with tyrosine phosphorylation of the E-cadherin/beta-catenin complex in cells transformed with a temperature-sensitive v-SRC gene. The Journal of cell biology. 1993;120(3):757-66.

34.   Guarino M. Src signaling in cancer invasion. Journal of cellular physiology. 2010;223(1):14-26.

35.   Angers-Loustau A, Hering R, Werbowetski TE, Kaplan DR, Del Maestro RF. SRC regulates actin dynamics and invasion of malignant glial cells in three dimensions. Molecular cancer research : MCR. 2004;2(11):595-605.

36.   Pohorelic B, Singh R, Parkin S, Koro K, Yang AD, Egan C, et al. Role of Src in breast cancer cell migration and invasion in a breast cell/bone-derived cell microenvironment. Breast cancer research and treatment. 2012;133(1):201-14.

37.   Tsao AS, He D, Saigal B, Liu S, Lee JJ, Bakkannagari S, et al. Inhibition of c-Src expression and activation in malignant pleural mesothelioma tissues leads to apoptosis, cell cycle arrest, and decreased migration and invasion. Molecular cancer therapeutics. 2007;6(7):1962-72.

38.   Tryfonopoulos D, Walsh S, Collins DM, Flanagan L, Quinn C, Corkery B, et al. Src: a potential target for the treatment of triple-negative breast cancer. Annals of oncology : official journal of the European Society for Medical Oncology. 2011;22(10):2234-40.

39.   Chang YM, Bai L, Liu S, Yang JC, Kung HJ, Evans CP. Src family kinase oncogenic potential and pathways in prostate cancer as revealed by AZD0530. Oncogene. 2008;27(49):6365-75.

40.   Fincham VJ, Frame MC. The catalytic activity of Src is dispensable for translocation to focal adhesions but controls the turnover of these structures during cell motility. The EMBO journal. 1998;17(1):81-92.

41.   Webb DJ, Donais K, Whitmore LA, Thomas SM, Turner CE, Parsons JT, et al. FAK-Src signalling through paxillin, ERK and MLCK regulates adhesion disassembly. Nature cell biology. 2004;6(2):154-61.

42.   Wozniak MA, Modzelewska K, Kwong L, Keely PJ. Focal adhesion regulation of cell behavior. Biochimica et biophysica acta. 2004;1692(2-3):103-19.

43.   Creedon H, Brunton VG. Src kinase inhibitors: promising cancer therapeutics? Critical reviews in oncogenesis. 2012;17(2):145-59.

Figure legends

Figure 1 EPLIN expression in prostate cancer cells lines, confirmation of EPLINα overexpression in PC-3 and LNCaP cells, and clinical tissue staining in normal prostate and prostate cancer. (A) PCR (left) and western blot (right) analyses of wild-type prostate cell lines showing EPLIN, EPLINβ and GAPDH expression in PC-3, DU-145, LNCaP, VCaP, PZ-HPV-7 and CA-HPV-10 cells. (B) Verification of EPLIN transcript (left) and protein (right) overexpression in the PC-3 cell model. (C) Verification of EPLIN transcript (left) protein (right) overexpression in the LNCaP cell model. Gel/blot images are representative of a minimum of three independent sample/repeats. For conciseness, composites are prepared using multiple gels/blots and representative GAPDH controls cropped and grouped together to represent overall trend. Comparative bands for individual molecules were taken from the same image. (D) EPLIN expression in normal prostate and in prostate cancer (TMA HPro-Ade96Sur-01). Representative images of EPLIN IHC staining from normal (n=8) and prostate cancer (n=36) samples at X20 objective magnification. (E) EPLIN expression in normal prostate, adjacent normal, chronic inflammation, hyperplasia and adenocarcinoma tissues (TMA PR8011a). Representative images of EPLIN IHC staining from normal prostate (n=8), adjacent normal (n=6), chronic inflammation (n=6), hyperplasia (n=26) and adenocarcinoma (n=30) tissue sections at X20 objective magnification. Respective boxplot representations show showing Median, Q1 and Q3 staining intensity scores and whiskers represent minimum and maximum staining intensity scores. ** = $p \leq 0.01$ and *** = $p \leq 0.001$.

Figure 2 *In vitro* functional impact of EPLINα overexpression on PC-3 and LNCaP prostate cancer cell lines. (A) *In vitro* tumour cell growth assay in PC-3^{pEF6} and PC-3$^{EPLIN\ EXP}$ cells at Day 3 and Day 5. (B) *In vitro* tumour cell growth

assay in LNCaP^{pEF6} and LNCaP$^{EPLIN\ EXP}$ cells at Day 3 and Day 5. (C) *In vitro* tumour cell invasion assay in PC-3^{pEF6} and PC-3$^{EPLIN\ EXP}$ cells. (D) *In vitro* tumour cell invasion assay in in LNCaP^{pEF6} and LNCaP$^{EPLIN\ EXP}$ cells. (E) *In vitro* tumour cell wound healing assay in PC-3^{pEF6} and PC-3$^{EPLIN\ EXP}$ cells. Experiment recorded over 4 hours at 1 hour intervals. Cellular migration compared to Time 0 for PC-3^{pEF6} and PC-3$^{EPLIN\ EXP}$ cells. (F) *In vitro* tumour cell transwell migration assay in in LNCaP^{pEF6} and LNCaP$^{EPLIN\ EXP}$ cells. Representative images for each experiment are shown. Bar charts represent mean of three independent repeats (n=3). Error bars represent SE of the Mean. * = p≤0.05, ** = p≤0.01.

Figure 3 EPLINα regulation of paxillin and FAK in prostate cancer and functional significance in combination with an FAK inhibitor (A) PCR quantification of FAK and paxillin transcript expression in PC-3/LNCaP^{pEF6} and PC-3/LNCaP$^{EPLIN\ EXP}$. (B) Western blot analysis of total FAK/paxillin expression and FAK/paxillin phospho-protein expression in control and EPLINα overexpression cell lines. Molecules screened were total FAK, p-FAK Y397, p-FAK Y925, total paxillin, p-paxillin Y31 and p-paxillin Y118. Gel/blot images are representative of a minimum of three independent samples/repeats. For conciseness, composites are prepared using multiple gels/blots and representative GAPDH controls cropped and grouped together to represent overall trend. Comparative bands for individual molecules were taken from the same image (C) Effect of FAK inhibition in combination with EPLINα overexpression on cellular invasion in PC-3 cells. (D) Effect of FAK inhibition in combination with EPLINα overexpression on cellular invasion in LNCaP cells. (E) Effect of FAK inhibition in combination with EPLINα overexpression on cellular migration in PC-3 cells. Experiment recorded over 4 hours at 1 hour intervals. Cellular migration compared to Time 0 for PC-3^{pEF6} and

PC-3^{EPLIN EXP} cells. (F) Effect of FAK inhibition in combination with EPLINα overexpression on cellular migration in LNCaP cells. FAK inhibition used at a concentration of 5µM. Experimental impact of FAK inhibition was run in conjunction with characterisation of EPLIN overexpression in PC-3 and LNCaP cells, hence values for untreated control and overexpression cells are presented again for comparison with equivalent cells treated with FAK inhibitor. Data represent mean of three independent repeats (n=3). Error bars represent SE of the Mean. * = $p \leq 0.05$, ** = $p \leq 0.01$, *** ≤ 0.001.

Figure 4 Identification and validation of EPLINα interaction with Src. (A) Changes in Src expression detected by the Kinexus protein microarray when EPLINα is overexpressed. Data was analysed using Globally Normalised Signal Intensity and using the Z-ratio. Significance was determined using the Z-ratio; a z-ratio of > 1.64 or < -1.64 was deemed statistically significant. (B) Validation of Src and p-Src expression in control and EPLINα overexpression PC-3 and LNCaP cell lines. Molecules verified were total Src, p-Src Y419 and p-Src Y530. Gel/blot images are representative of a minimum of three independent samples/repeats. For conciseness, composites are prepared using multiple gels/blots and representative GAPDH controls cropped and grouped together to represent overall trend. Comparative bands for individual molecules were taken from the same image. (C) Semi-quantitative analysis of p-Src Y419 expression in PC-3^{pEF6} and PC-3^{EPLIN EXP}. (D) Semi-quantitative analysis of p-Src Y530 expression in PC-3^{pEF6} and PC-3^{EPLIN EXP}. (E) Semi-quantitative analysis of p-Src Y530 expression in LNCaP^{pEF6} and LNCaP^{EPLIN EXP}. GAPDH was used alongside validation experiments as a control and to normalise protein expression. Bar charts represent mean of three independent repeats (n=3). Error bars represent SE of the Mean.* = $p \leq 0.05$, ** = $p \leq 0.01$.

Figure 5 Functional impact of EPLINα overexpression and Src inhibition on PC-3 and LNCaP cell migration and invasion. (A) PC-3 invasion assay with Src inhibitor. Representative images of PC-3^{pEF6} and PC-3$^{EPLIN\ EXP}$ cells with/without src inhibitor at concentration 500nM. (B) PC-3 migration/wound healing assay with Src inhibitor. Representative images of PC-3^{pEF6} and PC-3$^{EPLIN\ EXP}$ cells (x20 magnification) at 0 hour and 4 hours of scratch assay, with/without src inhibitor. (C) LNCaP invasion assay with Src inhibitor. Representative images of LNCaP^{pEF6} and LNCaP$^{EPLIN\ EXP}$ cells (x20 magnification) with/without src inhibitor. (D) LNCaP transwell migration assay with Src inhibitor. Representative images of LNCaP^{pEF6} and LNCaP$^{EPLIN\ EXP}$ cells with/without src inhibitor. Bar charts represent mean of three independent repeats (n=3). Error bars represent SE of the Mean.* = represents $p \leq 0.05$, ** = $p \leq 0.01$ and *** = $p \leq 0.001$.

Figure 6 EPLIN knockdown using shRNA in CA-HPV-10 cells and associations with paxillin, FAK and Src. (A) Verification of EPLIN transcript knockdown by PCR. Semi-quantitative analysis shown using Image J software and knockdown depicted as % control. (B) Verification of EPLIN protein knockdown by western blotting. Semi-quantitative analysis shown using Image J software and knockdown depicted as % control. (C) Western blot of the effect of EPLIN knockdown in CA-HPV-10 on the expression of paxillin, paxillin Y31 and paxillin Y118. (D) Western blot of the effect of EPLIN knockdown in CA-HPV-10 on the expression of total FAK, FAK Y397, FAK Y925. (E) Western blot of the effect of EPLIN knockdown in CA-HPV-10 on the expression of total Src, Src Y419, Src Y530. Gel/blot images are representative of a minimum of three independent samples/repeats. For conciseness, composites are prepared using multiple gels/blots and representative GAPDH controls cropped and grouped together to represent overall trend.

Comparative bands for individual molecules were taken from the same image. (F) Effect of EPLIN knockdown in conjunction with FAK or Src inhibition on CA-HPV-10 cellular invasion. (G) Effect of EPLIN knockdown in conjunction with FAK or Src inhibition on CA-HPV-10 cellular migration. Bar charts shown represent mean values of a minimum of three independent repeats. Error bars represent SE of the Mean. * p = $\leq$0.05, ** p = $\leq$0.01, *** p = $\leq$0.001.

Supplementary Figure 1 EPLIN Gene Expression Omnibus (GEO) profiles and EPLIN IHC staining of EPLIN corresponding the cancer stage and Gleason score. (A) Profile GDS2865 / 217892_s_at; EPLIN score value in poorly metastatic tissue and highly metastatic tissue (top). Profile GDS1439 / 222457_s_at; EPLIN score value in benign prostate tissue, primary prostate cancer and metastatic prostate cancer (bottom). Cohorts extracted from NCBI GEO database. (B) Boxplot representations showing Median, Q1 and Q3 staining intensity. Box plot data shows Stage II (n=7) vs. combined Stage III and IV (n=29). Whiskers represent minimum and maximum staining intensity. (C) Boxplot representations of Median, Q1 and Q3 staining intensity scores. Box plot data shows combined Gleason 6/7 (n=14) vs. combined Gleason 8/9/10 (n=22). Whiskers represent minimum and maximum staining intensity. * = represents p$\leq$0.05, ** = p$\leq$0.01 and *** = p$\leq$0.001.

Supplementary Figure 2 Semi-quantitative analysis of western blot protein bands shown in Figure 3 with significant differences following EPLIN overexpression. (A) pFAK Y925 expression in PC-3^{pEF6} and PC-3$^{EPLIN\ EXP}$ cells following semi-quantitative analysis and normalisation to GAPDH. (B) Paxillin Y31 expression in PC-3^{pEF6} and PC-3$^{EPLIN\ EXP}$ cells following semi-quantitative analysis and normalisation to GAPDH. (C) Paxillin expression in PC-3^{pEF6} and PC-3$^{EPLIN\ EXP}$ cells following semi-quantitative analysis and normalisation to GAPDH. (D)

pPaxillin Y118 expression in PC-3^{pEF6} and PC-3$^{EPLIN\ EXP}$ cells following semi-quantitative analysis and normalisation to GAPDH. (E) pFAK Y397 expression in LNCaP^{pEF6} and LNCaP$^{EPLIN\ EXP}$ cells following semi-quantitative analysis and normalisation to GAPDH. (F) pPaxillin Y118 expression in LNCaP^{pEF6} and LNCaP$^{EPLIN\ EXP}$ cells following semi-quantitative analysis and normalisation to GAPDH. Bar charts represent the mean average of band intensity of three independent repeats (n=3). Error bars represent SE of the Mean. * = p≤0.05, ** = p≤0.01 and *** = p≤0.001.

Supplementary Figure 3 Semi-quantitative analysis of western blot protein bands shown in Figure 6 with significant or notable differences following EPLIN knockdown. (A) FAK expression in CA-HPV-10 cells transfected with control shRNA or EPLIN shRNA following semi-quantitative analysis and normalisation to GAPDH. (B) FAK Y397 expression in CA-HPV-10 cells transfected with control shRNA or EPLIN shRNA following semi-quantitative analysis and normalisation to GAPDH. (C) Src Y419 expression in CA-HPV-10 cells transfected with control shRNA or EPLIN shRNA following semi-quantitative analysis and normalisation to GAPDH. Bar charts shown represent mean values of a minimum of three independent repeats. Bar charts are represented as percentage/control. Error bars represent SE of the Mean. * = p≤0.05, ** = p≤0.01 and *** = p≤0.001.

Figure 1

(A)

(B)

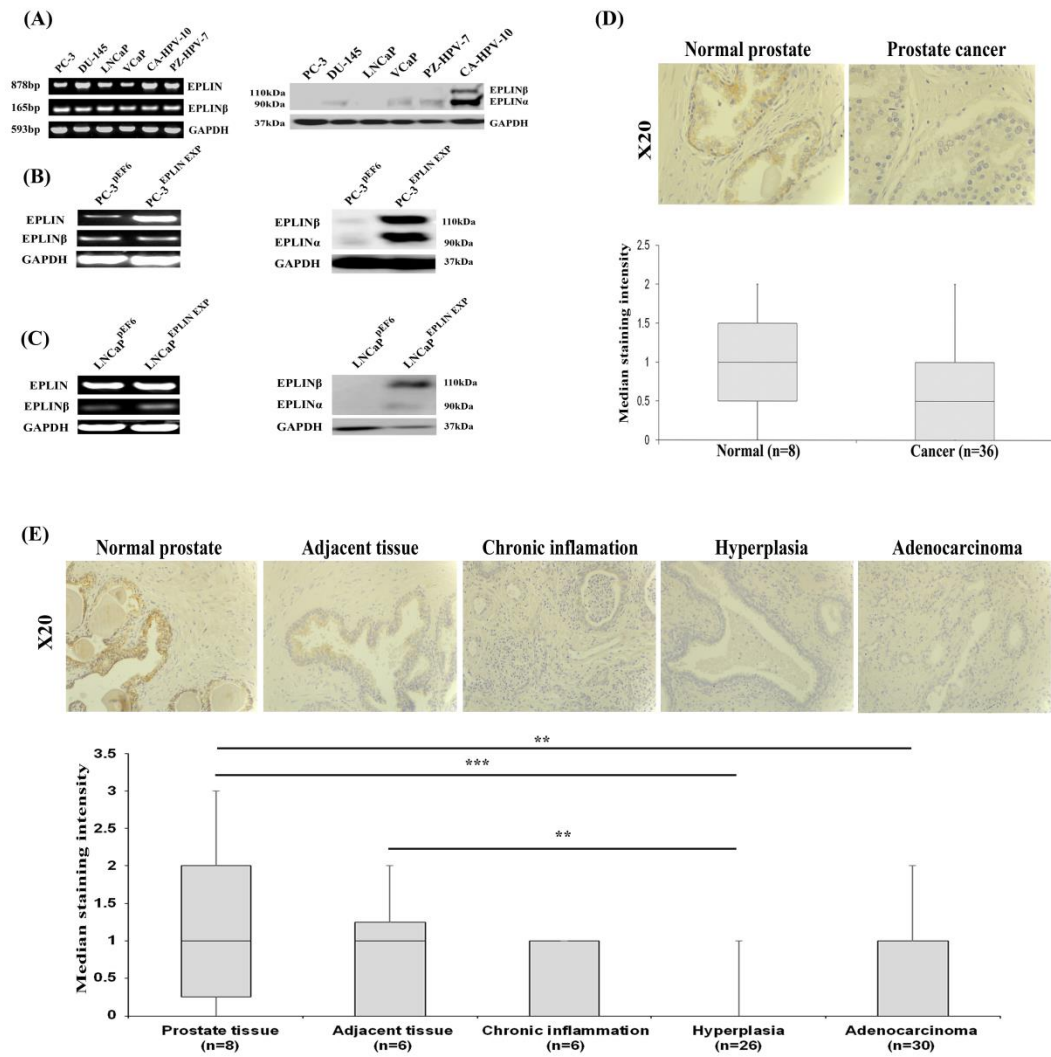**(C)**

(D)

Normal prostate   Prostate cancer

X20

(E)

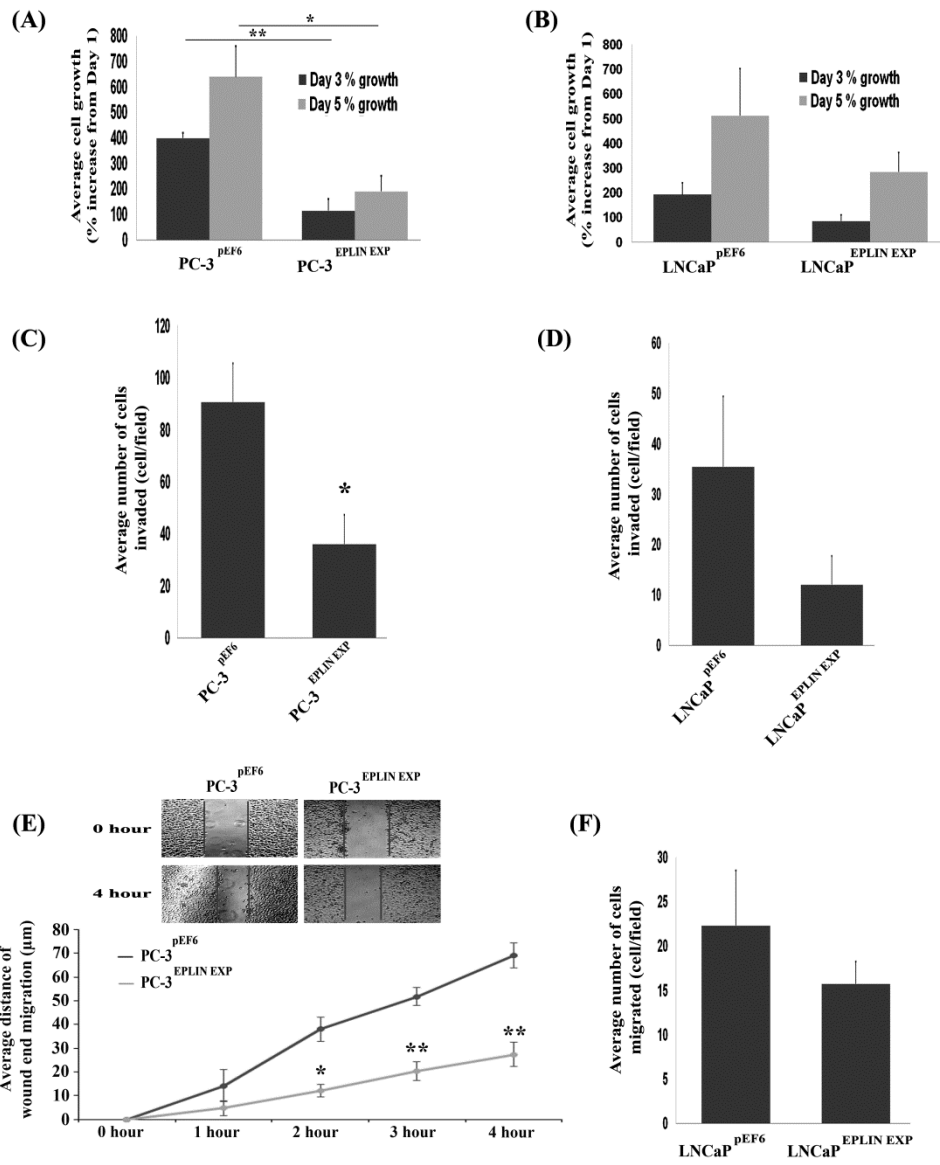Normal prostate   Adjacent tissue   Chronic inflamation   Hyperplasia   Adenocarcinoma

X20

Figure 2

Figure 3

Figure 4

(A)

(B)

PC-3 pEF6   PC-3 EPLIN EXP   LNCaP pEF6   LNCaP EPLIN EXP

Total Src   60kDa
Src Y419   60kDa
Src Y530   60kDa
GAPDH   37kDa

(C)   (D)   (E)
Src Y419 expression in PC-3   **Src Y530 expression in PC-3**   **Src Y530 expression in LNCaP**
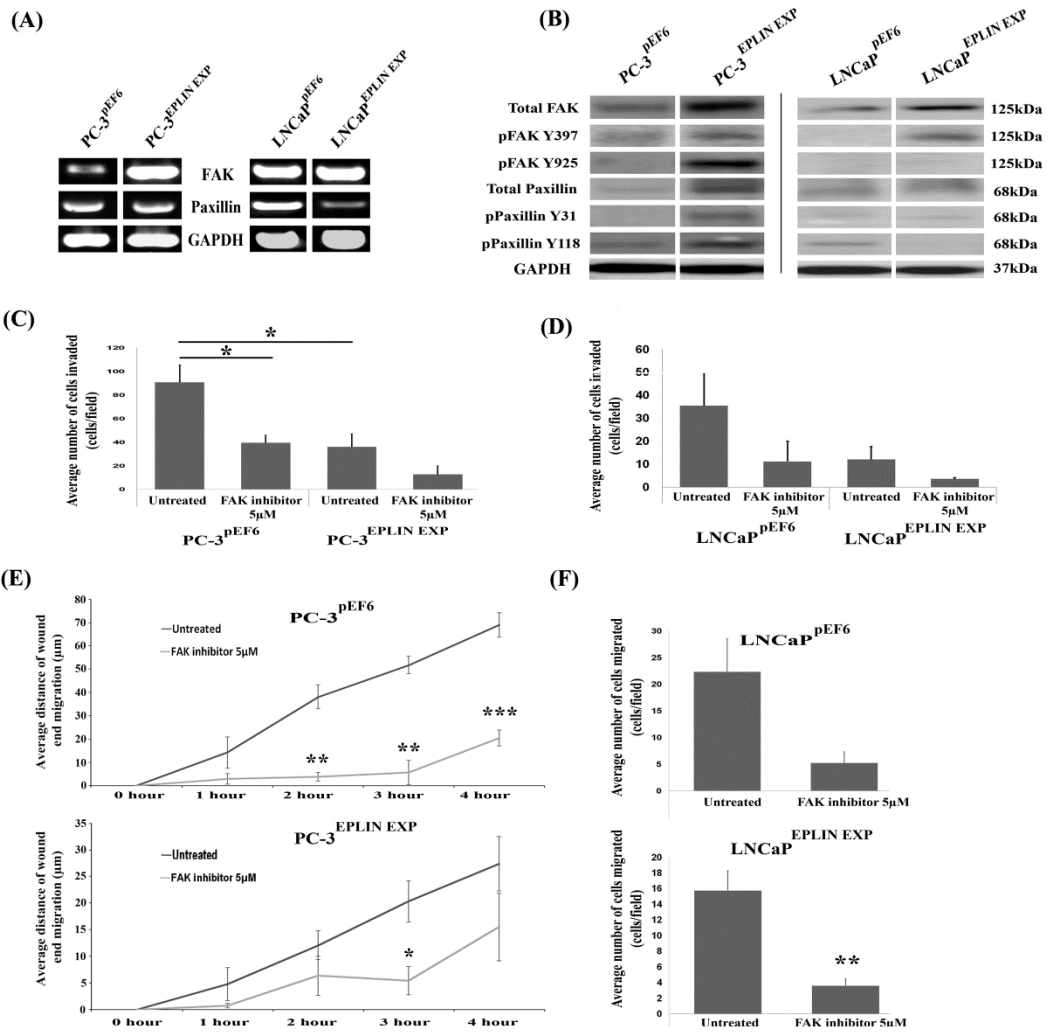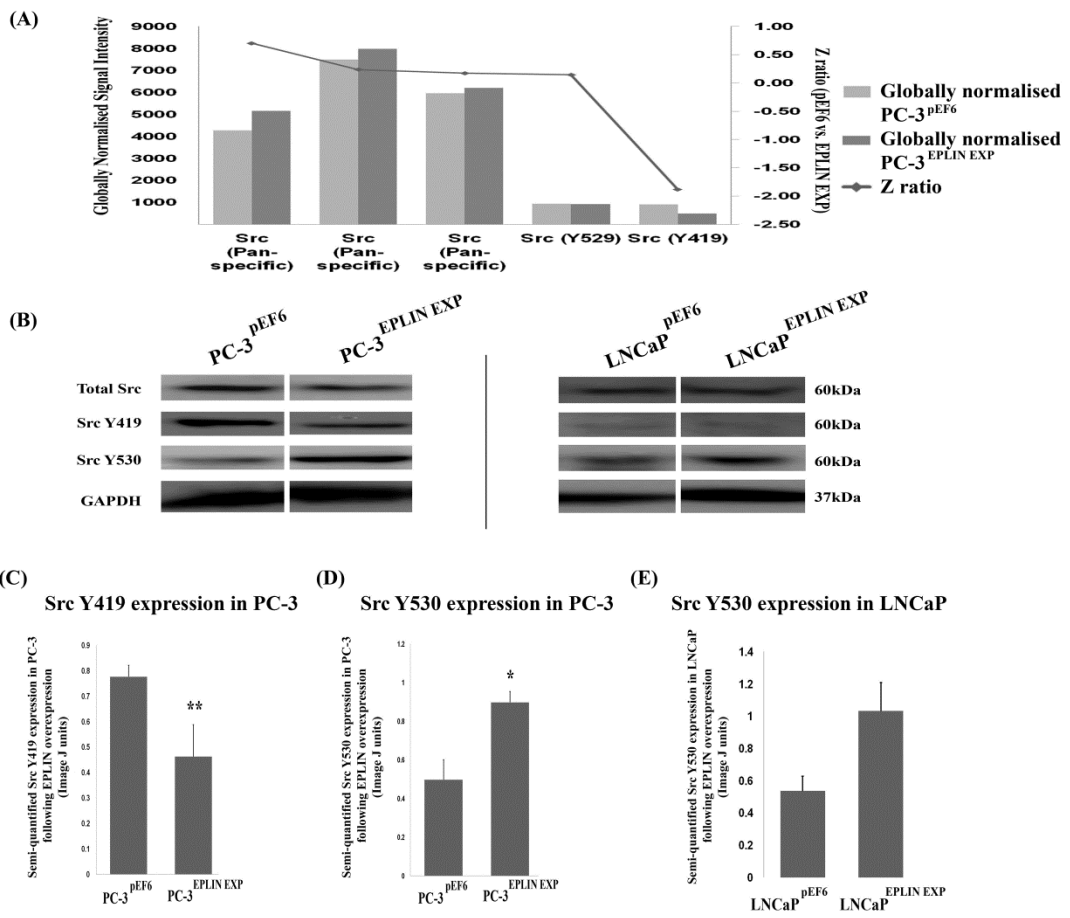
Figure 5

Figure 6

Sup Fig 1

Sup Fig 2

(A)

pFAK925 expression

(B)

pPaxillin Y31 expression

(C)

Paxillin expression

(D)

pPaxillin Y118 expression

(E)

pFAK Y397 expression
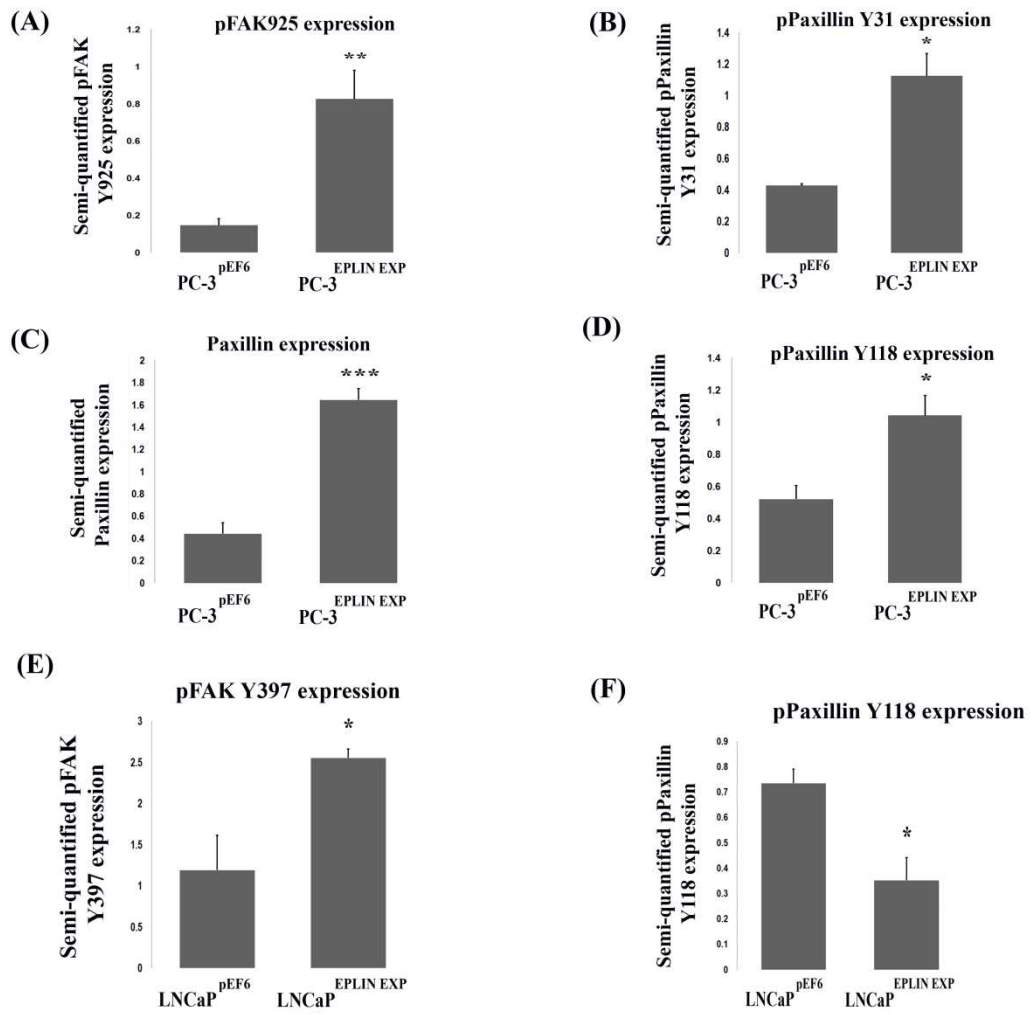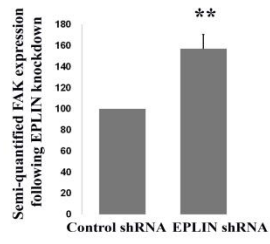

(F)

pPaxillin Y118 expression
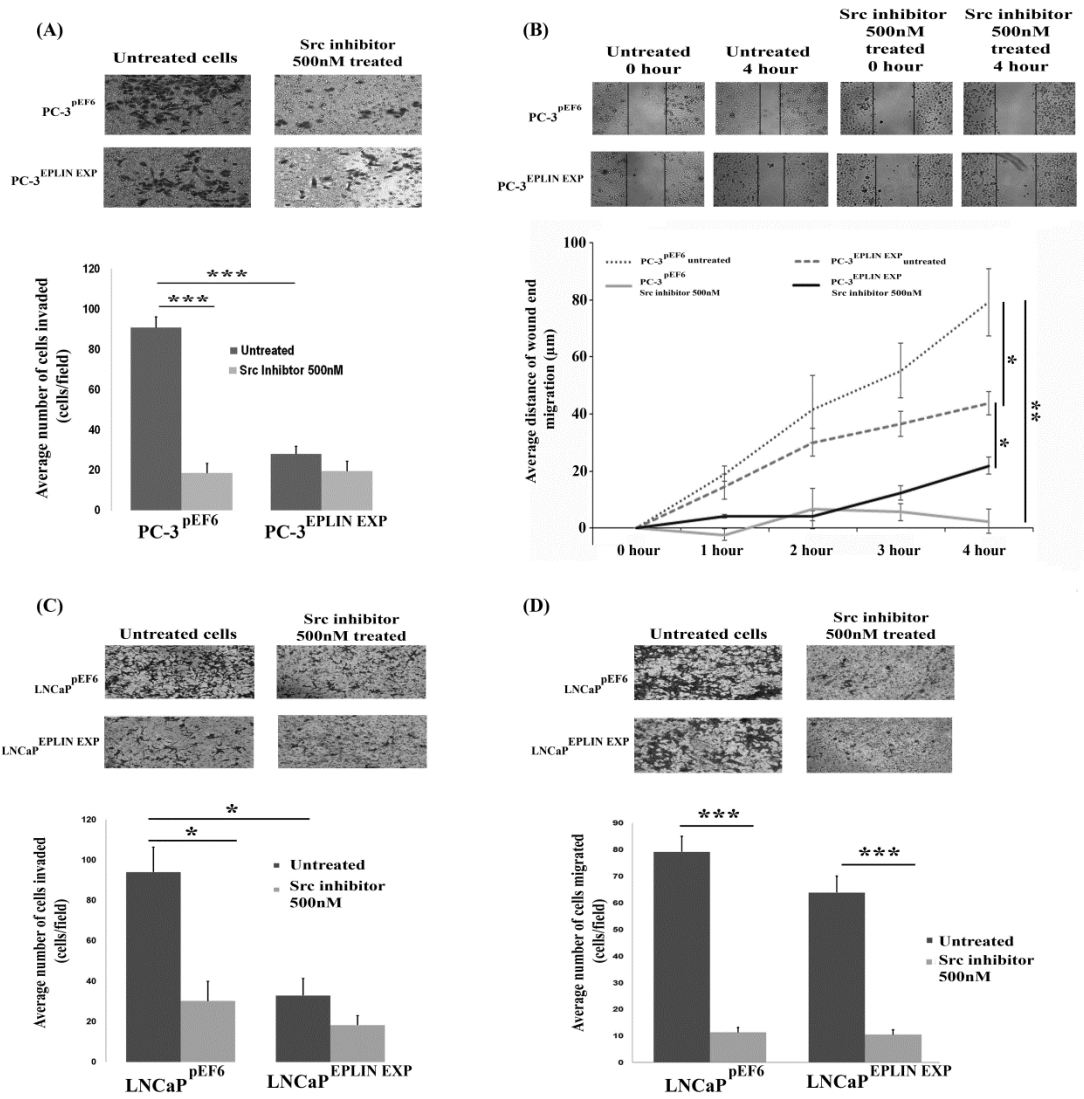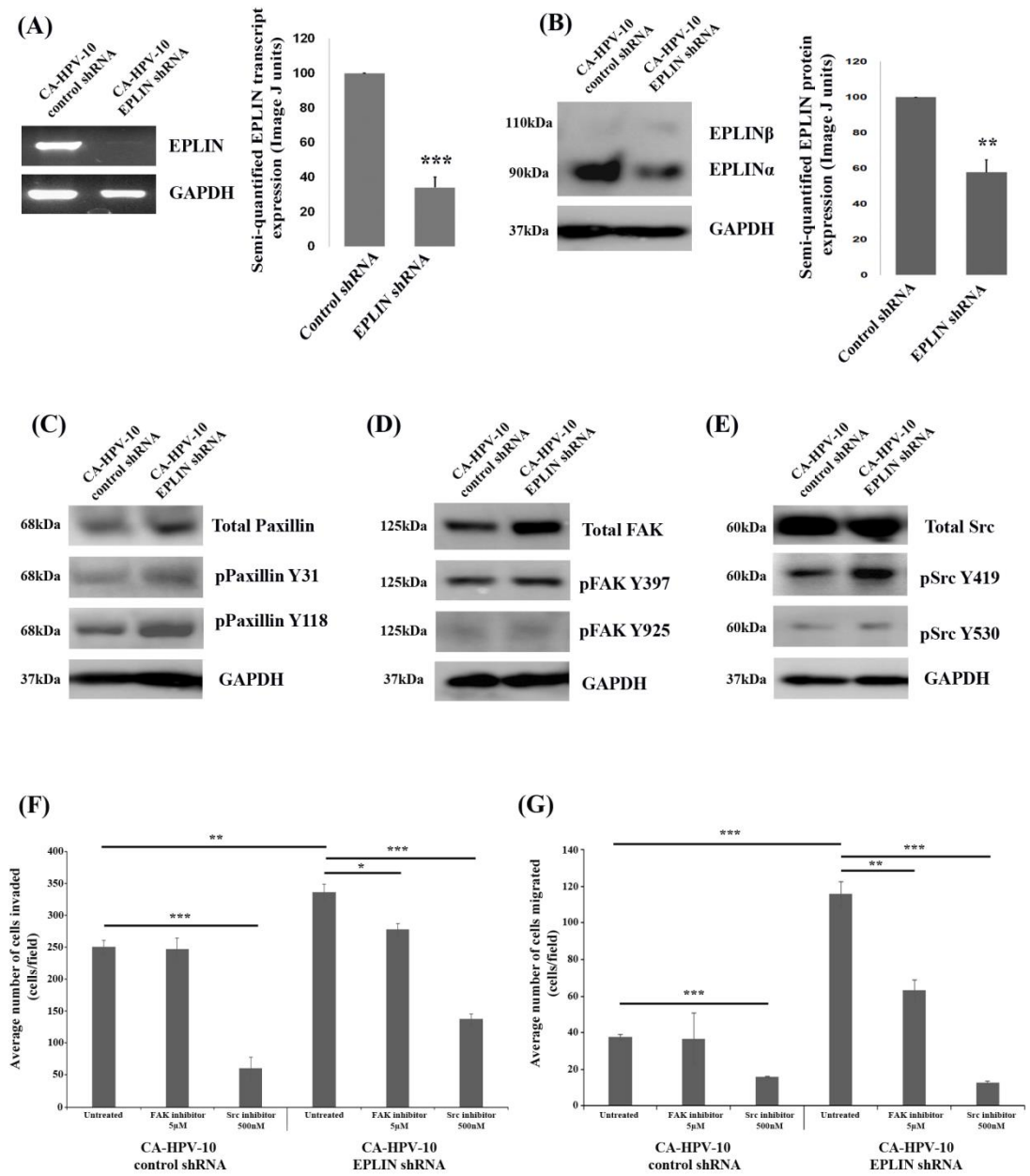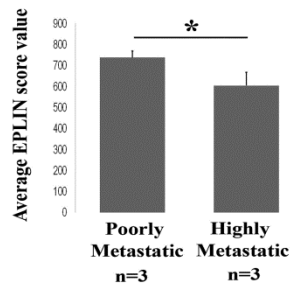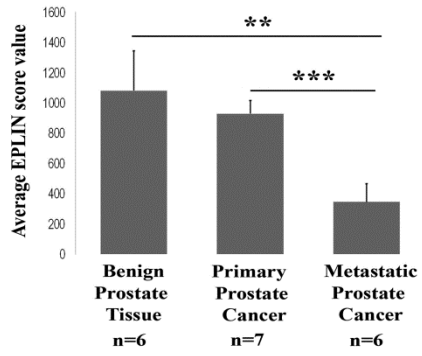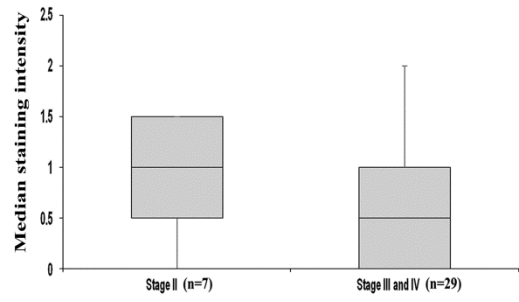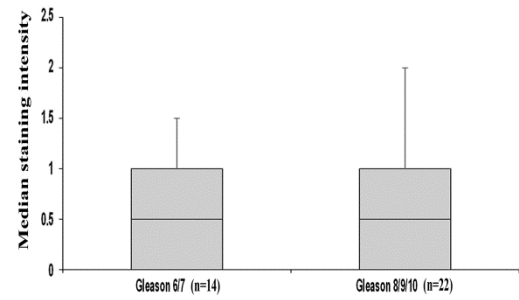
Sup Fig 3

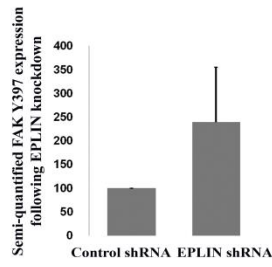**(A)** Total FAK expression in CA-HPV-10

(B) FAK Y397 expression in CA-HPV-10

(C) Src Y419 expression in CA-HPV-10